Supplementary Information

Unexpected higher corrosion in the gas phase region of metals caused by calcium and magnesium ions than sodium ions

Authors: Yi Luo[1]†, Zhenglin He[1]†, Huayan Yang[1], Yunzhang Li[1], Dongting Yue[1], Zehui Zhang[1], Guosheng Shi[1,2*]

Affiliations: [1]Shanghai Applied Radiation Institute, State Key Lab. Advanced Special Steel, Shanghai University, NO.99 Shangda Road, Baoshan District, Shanghai 200444, China

[2]Key Laboratory of Comprehensive and Highly Efficient Utilization of Salt Lake Resources, Qinghai Institute of Salt Lakes, Chinese Academy of Sciences, Xining, Qinghai 810008, PR China.
*Correspondence to: gsshi@shu.edu.cn (G.S.)

†These authors contributed equally to this work.

Table of contents

Section 1: Experiments

1.1 Materials

Ultrapure deionized water (Milli-Q, Millipore, 18.2 MΩ·cm resistivity) was used in the whole process, which was purchased from Shanghai Rephile Bioscience

Con, Ltd. The iron sheet (φ 20mm×1mm) of 99.999% (Fe 99.999%, C 0.0005%, Si 0.0002%, Mn 0.0003%) purity was bought from North China Science and Technology Metal Materials Co., Ltd. Magnesium chloride ($MgCl_2$, purity > 99.9%), Magnesium chloride hexahydrate (MgCl2, purity > 99.9%), sodium chloride (NaCl, purity > 99.9%), Acetone (CH3COCH3, purity > 99.5%), epoxy resin E-44 and anhydrous ethanol (C2H5OH, purity > 99.7%) all were purchased from Shanghai Titan Scientific Co., Ltd. Sandpaper with silicon carbide (SiC) and Alumina (Al2O3) polishing powder as the main materials was purchased from Shanghai Difeng New Material Co., Ltd.

1.2 Preparation of iron samples

Pure iron samples were grinded by using different sizes of silicon carbide (SiC) abrasive papers 240#, 400#, 1000#, 1500#, 2000#, consecutively. The iron sample was polished at 100RPM for one minute by the polishing powder with aluminum oxide (Al_2O_3 with a diameter of 0.1um to mixed with Ultrapure water by a 1:5 ratio) as the main component. We cleaned the impurities on the surface with deionized water and the polished samples was wiped by dust free paper, then put it into a micro ultrasonic machine contains with anhydrous ethanol and acetone[1, 2], take it out after ultrasonic for about 5 minutes, dry it with nitrogen, and place it in desiccators for future use.

1.3 Preparation of 0.04 M $MgCl_2$ and 0.6 M NaCl solution

The 100 ml solvents are made up of anhydrous ethanol (C_2H_5OH, purity > 99.9%) proportions from 0, 25, 50, 75 to 100 vol.%, plus Ultrapure water (Milli-Q, Millipore, 18.2 MΩ·cm resistivity). Magnesium chloride ($MgCl_2$, purity > 99.9%) was weighed at 0.38g on the electronic analysis balance, the weighed $MgCl_2$ was slowly poured into the prepared 100 ml volumetric bottle and add pure water to 100 ml, and the remaining four groups of solvent configurations with different alcohol-water ratios were repeated successively. The five groups of solvent configurations worked in a dry and clean glass at a speed of 500 RPM under the work of a magnetic stirrer for 1 h.

Sodium chloride (NaCl, purity > 99.9%) is slightly soluble ethanol, thus it's going to be weighed into five different masses of solutes, including1.75g, 0.43g, 0.87g, 1.31g and 1.75g, by reason of the ratio from 0, 25, 50, 75 to 100 vol.% ethanol. Finally, magnesium chloride and sodium chloride solution are concentration of 0.04 M and 0.6 M respectively. The concentration selected in this experiment is based on the magnesium and sodium salt content in seawater, which quality fraction are 3.5% and 0.23%, respectively.

1.4 Half immersion test in $MgCl_2$ and NaCl solution

The 2.5 ml 0.04 M $MgCl_2$ and 0.6 M NaCl solution, which is same as the concentration of magnesium and sodium salt in seawater, was respectively added to the 10 ml beaker for ensure that the liquid level covers the half of the iron surface in the gas-liquid experiment. The solvent is configured with different proportions of ethanol, and anhydrous ethanol rations increasing from 0, 25, 50, 75 to 100 vol.%. The experimental conditions were the ambient conditions. The prepared iron samples should be cleaned and dried before use. The unpolished side of the iron sample is coated with epoxy resin to reduce the influence of uncontrollable factors. The experiment is the humidity controlled at 50 ± 5% and temperature maintained at 25 ± 1.5°C, samples were observed simultaneously at intervals of about 1 h each time. The end point of the experiment is the complete volatilization of 100 vol.% ethanol about 6 h. All experiments were repeated in three groups under similar conditions.

1.5 Half immersion test in $CaCl_2$ and $BaCl_2$ solution

With reference to the concentration of barium and calcium ions (Ca^{2+}: 410 mg/L; Ba^{2+}: 0.05 mg/L) in seawater, the concentration of $CaCl_2$ solution is 0.01 M and $BaCl_2$ is 0.03×10^{-5} M**.** Under the same conditions, the circular iron samples were semi-immersed in the two systems.

1.5 The digital photos and optical microscope of corrosion areas

In this experiment, the end point was the complete volatilization of the 2.5 ml 100 vol.% anhydrous ethanol in the beaker, which took about 6 h. and the corrosion

effect was observed by sample every 1 h. After the absolute ethanol was completely volatilized, five groups of iron samples, which were half-immersed in 0.04 M $MgCl_2$ solution with different ethanol ratios, were immediately taken out and blown dry with nitrogen for comparison, and the final corrosion morphology was recorded with a digital camera (Canon, EOS 80) for analysis changes of corroded iron[3, 4]. Similarly, the corrosion morphology was recorded for a half-immersed solution containing 0.6 M NaCl solution containing different proportions of ethanol. Meanwhile, the morphology of the corrosion area was recorded by optical microscopy.

1.6 Weight loss test

Standard 10 sets of square iron sheet ($1\times1cm^2$) specimens were selected for weight loss testing. The iron sheets were polished by 1000# sandpaper and then sonicated in a micro-ultrasonic cleaner containing ethanol, and subsequently removed and set aside in a vacuum drying oven. The mass of the processed iron sheet was recorded as m_0 (0.65719g). The processed iron sheet was placed vertically in a standard 10 ml beaker (7.70221g), and 2.3 ml of the solution was added to semi-immersed the iron sheet to observe the phenomenon of corrosion weight. The end point was the volatilization of 100 vol.% ethanol, and the solution was continuously added, and the number of cycles was recorded as N to ensure that the corrosion behavior continued. After N=10, the final mass of the iron sheet and beaker together was recorded as m_n, and we defined the corrosion rate as $V= (m_{n-} m_0)/St$ ($g.cm^{-2}.h^{-1}$).

The polished and prepared iron sheets were weighed as m_0. The circular iron sheet specimens were semi-immersed in 0.04 M $MgCl_2$ solution and 0.6 M NaCl solution. The evaporation of 100% ethanol as the number of cycles, the solution was continuously added to ensure the corrosion behavior was sustained. The weight of the corroded iron sheet was recorded m_n. The Δm was defined as m_n-m_0, which was used measure the distinction of corrosion in the different two systems.

1.6 Characterization of corrosion areas

The photoshop software was used to measure the area of corroded iron sample in

the recorded photos. Here, we define the percentage of corroded area (R_A= Scorrosion/Stotal) is the corroded area divided by area of the entire iron sheet. Since the diameter of the pure iron sample is known to be 2 centimeters, we defined the ratio of pixels to centimeters to be 188:1 in photos recording the iron half-immersed in 0.04 M $MgCl_2$ solution and the other scale is 256:1 in 0.6 M NaCl solution. The selected areas were calculated by Magic wand tool in photoshop software. In the corrosion products caused by $CaCl_2$ and $BaCl_2$ solution, the ratio of pixels to centimeters to be 251:1.

1.7 Characterization of corrosion products

In order to compare the difference of corrosion microstructure caused by water salt and anhydrous ethanol solution. Scanning electron microscopy (LEO 1530VP, Zeiss SEM operated at 15 kV, working distance at 6~8mm) was used to observe different corrosion products in the liquid phase and gas phase. The X-ray diffraction (XRD, Bruker, 08DISCOVER, λ=0.15418 nm, working voltage = 18 kV, current = 40 mA) was used to determine the composition of iron oxides in corrosion products. Under the 15kv electron energy, scanning electron microscopy-energy dispersive spectroscopy (SEM-EDS) was used to analyze the oxygen content and chemical elements in corrosion products, including the liquid phase, gas phase and the gas-liquid interface, to quantitatively characterize corrosion caused by magnesium salts containing different ratios of ethanol. The X-ray Photoelectron Spectroscopy (XPS, source gun type, Al K Alpha; ion energy, 1486.6 eV; current, 6 mA; spot size, 400μm; background subtraction, smart; vacuum, 3×10^{-8} mbar; scan mode, CAE; depth probed,1~10 nm.) was characterized the composition of corrosion products in the gas phase. In the $MgCl_2$ solution containing 100 vol.% ethanol, the circular iron specimens were sent to the FT-IR spectrometer for testing, when they appeared as foggy liquid in the gas phase region. The resolution of the infrared spectrum analyzer was 4 cm^{-1}, the number of scans was 32, and the scanning range was 400-4000 cm^{-1}.

1.8 Electrochemical impedance spectroscopy of the liquid phase in the 0.04 M

$MgCl_2$.

A 760E electrochemical workstation (Corrtest Instruments, China) was employed to conduct electrochemical measurements by using a three-electrode cell. Electrochemical experiments were carried out in a test solution containing 100 ml 0.04 M $MgCl_2$ solution. The solvents used in this experiment are alcohols with 0, 25, 50, 75 and 100 vol.%. A graphite electrode and a saturated calomel electrode were used as the counter electrode and reference electrode. The open-circuit potential (OCP) was stabilized in different solutions for 1 h before all experiments began. In the EIS, the frequency range was: 1000KHz to 0.01Hz,[5] and the amplitude was 5 mV (peak to peak) using AC signals at OCP.

1.9 Polarization curves of the liquid phase in the 0.04 M $MgCl_2$ and 0.6 M NaCl.

Polarization curve tests were performed. The polarization curves were obtained at a constant scan rate of 5 mV/s. The open-circuit potential relative to the self-corrosion potential ranged from -1200 mV to +500 mV for the $MgCl_2$ solution, and the open-circuit potential relative to the self-corrosion potential is -1200mV ~ +200mV for the NaCl solution.

Section 2: The polised iron sample and experimental results

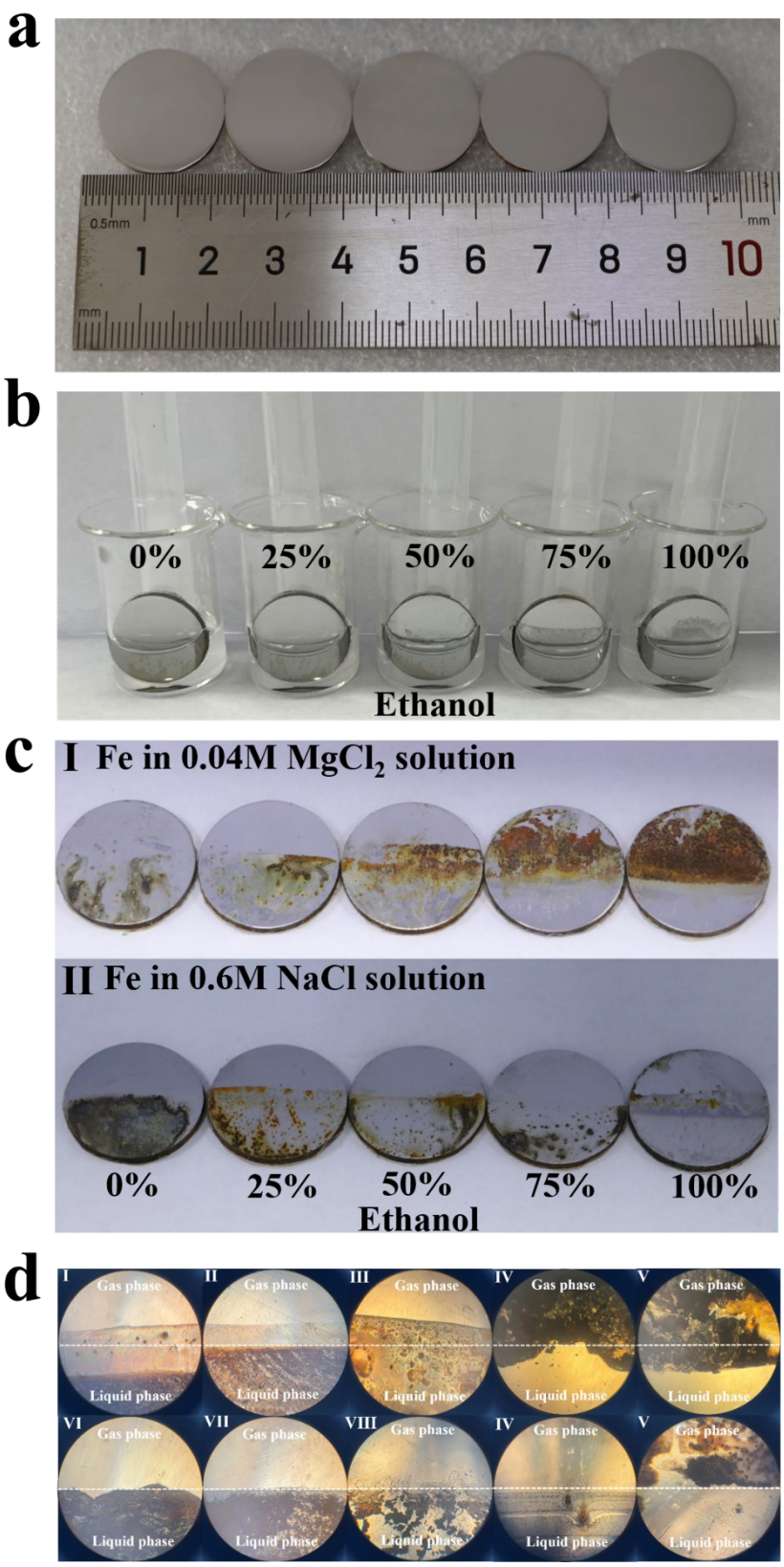

Supplementary Fig. 1 | (a) Digital photos of polished iron sample. (b) Experimental figure of iron semi-immersed in solutions containing ethanol ratio from 0, 25, 50, 75 to 100 vol.%, respectively. (c) Original digital photograph of iron samples that being semi-immersed in 0.04 M $MgCl_2$ and 0.6 M NaCl solutions for 6 h. (Solutions contain different ethanol rations from 0, 25, 50, 75 to 100 vol.%, respectively). c(I), iron was semi-immersed in 0.04 M $MgCl_2$ solution, c(II) iron was semi-immersed in 0.6 M NaCl solution. (d) Microscopic photographs of corroded iron sheets: (I-V) Iron sheets semi-immersed in 0.04 M $MgCl_2$ solution; (VI-V) Iron sheets semi-immersed in 0.6 M NaCl solutions.

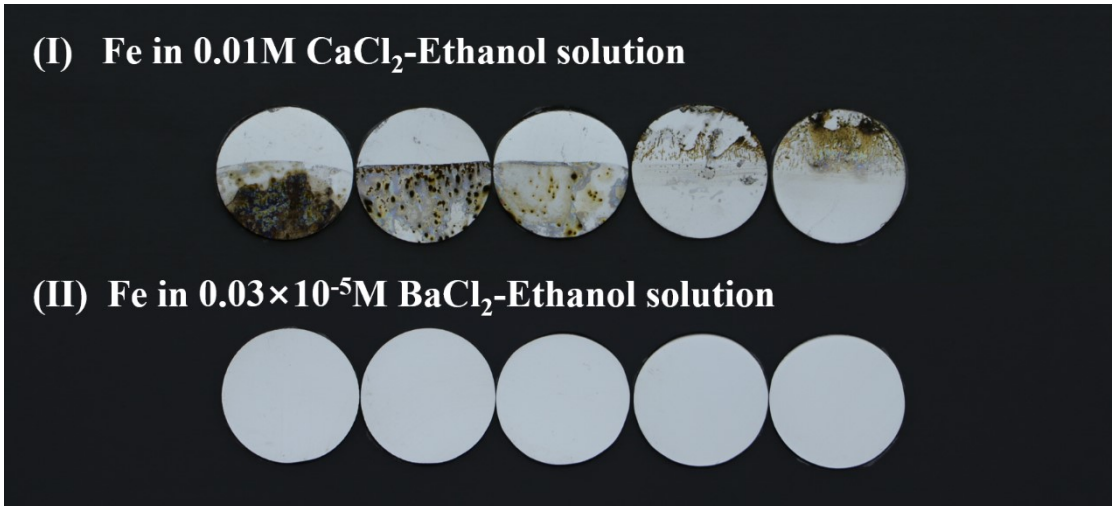

Supplementary Fig. 2 | Original digital photograph of iron samples that being semi-immersed in 0.01M $CaCl_2$ and 0.03×10^{-5} M $BaCl_2$ solutions for 6 h. (Solutions contain different ethanol rations from 0, 25, 50, 75 to 100 vol.%, respectively). c(I), iron was semi-immersed in 0.01 M $CaCl_2$ solution, c(II) iron was semi-immersed in 0.03×10^{-5}M $BaCl_2$ solution.

Section 3: The data of corrosion areas in the gas phase

The formula for the rations[6] of corrosion areas in the gas phase as:

(R_A=Scorrosion/Stotal)

Table 1:

The percentage of corrosion areas in the gas phase by 0.04 M $MgCl_2$ solution

Ethanol rations:	0%	25%	50%	75%	100%
1(%)	0	0	26.89	78.91	91.53
2(%)	0	0	28.12	79.89	92.73
3(%)	0	0	25.85	80.33	91.30

Average:	0	0	26.95	79.71	91.85
Errors:	0	0	0.92	0.59	0.62

Supplementary Table 1 | The percentage of corrosion areas in the gas phase caused by 0.04 M $MgCl_2$ solution containing ethanol rations from 0, 25, 50, 75 to 100 vol.%, respectively, in **Supplementary Fig. 1 c(I).**

Table 2:

The percentage of corrosion areas in the gas phase by 0.6 M NaCl solution

Ethanol rations:	**0%**	**25%**	**50%**	**75%**	**100%**
1(%)	0	0	0	0	3.01
2(%)	0	0	0	0	2.10
3(%)	0	0	0	0	3.61
Average:	0	0	0	0	2.91
Errors:	0	0	0	0	0.62

Supplementary Table 2 | The percentage of corrosion areas in the gas phase caused by 0.6 M NaCl solution containing ethanol rations from 0, 25, 50, 75 to 100 vol.%, respectively, in **Supplementary Fig. 1 c(II).**

Table 3:

The percentage of corrosion areas in the liquid phase by 0.04 M $MgCl_2$ solution

Ethanol rations:	**0%**	**25%**	**50%**	**75%**	**100%**
1(%)	39.57	39.84	28.77	0	0
2(%)	39.49	36.47	27.88	0	0
3(%)	40.97	34.03	26.34	0	0
Average:	40.01	36.78	27.66	0	0
Errors:	0.01	0.03	0.01	0	0

Supplementary Table 3 | The percentage of corrosion areas in the liquid phase caused by 0.04 M $MgCl_2$ solution containing ethanol rations from 0, 25, 50, 75 to 100 vol.%, respectively.

Table 4:

The percentage of corrosion areas in the liquid phase by 0.6 M NaCl solution

Ethanol rations:	**0%**	**25%**	**50%**	**75%**	**100%**
1(%)	78.68	58.94	38.43	25.73	0
2(%)	79.37	62.35	45.17	27.27	0
3(%)	80.10	64.52	42.72	28.31	0
Average:	79.38	61.94	42.11	27.10	0
Errors:	0.01	0.03	0.04	0.01	0

Supplementary Table 4 | The percentage of corrosion areas in the liquid phase caused by 0.6 M NaCl solution containing ethanol rations from 0, 25, 50, 75 to 100 vol.%, respectively.

Table 5:

The percentage of corrosion areas in the gas phase by 0.01 M $CaCl_2$ solution

Ethanol rations:	0%	25%	50%	75%	100%
1(%)	0	0	0	56.86	84.34
2(%)	0	0	0	56.68	85.72
3(%)	0	0	0	54.99	86.14
Average:	0	0	0	56.17	85.4
Errors:	0	0	0	1.03	0.94

Supplementary Table 5 | The percentage of corrosion areas in the gas phase caused by 0.01 M $CaCl_2$ solution containing ethanol rations from 0, 25, 50, 75 to 100 vol.%, respectively.

Table 6:

The percentage of corrosion areas in the liquid phase by 0.01 M $CaCl_2$ solution

Ethanol rations:	0%	25%	50%	75%	100%
1(%)	67.10	56.98	39.98	0	0
2(%)	69.44	58.12	41.97	0	0
3(%)	65.60	56.30	43.22	0	0
Average:	67.38	57.13	41.72	0	0
Errors:	0.02	0.03	0.01	0	0

Supplementary Table 6 | The percentage of corrosion areas in the gas phase caused by 0.01 M $CaCl_2$ solution containing ethanol rations from 0, 25, 50, 75 to 100 vol.%, respectively.

Table 7:

The percentage of corrosion areas in the gas-liquid interface by 0.01 M $CaCl_2$ solution

Ethanol rations:	0%	25%	50%	75%	100%
1(%)	65.86	56.08	43.78	66.26	84.14
2(%)	66.46	55.38	42.60	65.06	83.53
3(%)	67.16	53.27	41.96	66.67	82.12
Average:	66.49	54.91	42.78	65.99	83.26
Errors:	0.01	0.01	0.02	0.04	0.05

Supplementary Table 7 | The percentage of corrosion areas in the gas-liquid interface caused by 0.01 M $CaCl_2$ solution containing ethanol rations from 0, 25, 50, 75 to 100 vol.%, respectively.

Table 8:

The percentage of corrosion areas in the all phases by $0.03x10^{-5}$ M $BaCl_2$ solution

Ethanol rations:	0%	25%	50%	75%	100%

1(%)	0	0	0	0	0
2(%)	0	0	0	0	0
3(%)	0	0	0	0	0
Average:	0	0	0	0	0
Errors:	0	0	0	0	0

Supplementary Table 8 | The percentage of corrosion areas in the all phase caused by $0.03x10^{-5}$ M $BaCl_2$ solution containing ethanol rations from 0, 25, 50, 75 to 100 vol.%, respectively.

Section 4: The weight loss and Tafel data

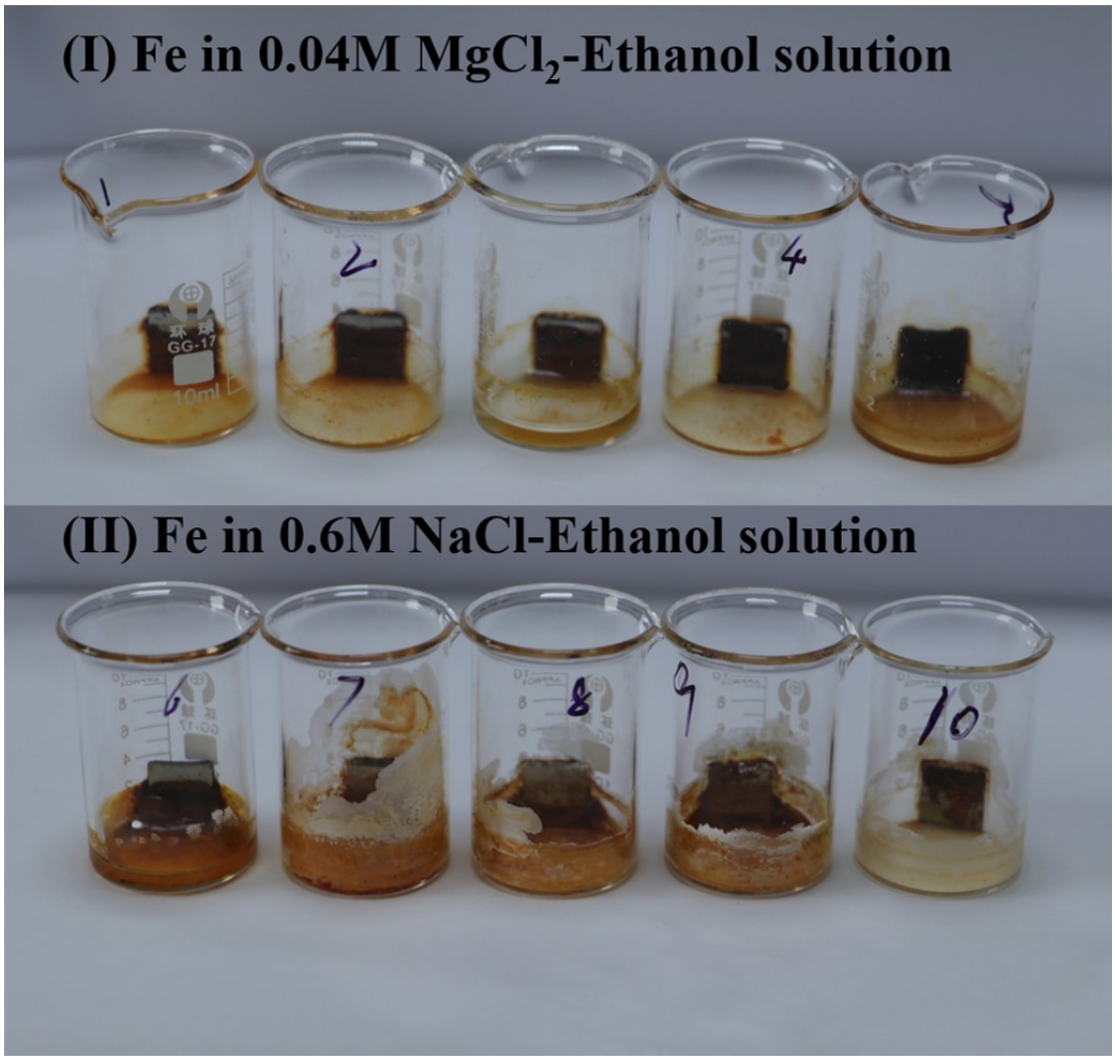

Supplementary Fig. 3 | (I) the weight loss of iron in the 0.04 M $MgCl_2$ solution, Corresponding respectively to 0, 25, 50, 75 and 100 vol.% ethanol. (II) the weight loss of iron in the 0.6 M NaCl solution, Corresponding respectively to 0, 25, 50, 75 and 100 vol.% ethanol.

The formula of the iron corrosion rate:

$$V = (m_n - m_0)/St \ (g.cm^{-2}.h^{-1})$$

m_n: The mass of corroded iron sheet and beaker

m_0: The mass of processed iron sheet and beaker

S: The area of square iron sheet

t: The time of ending corrosion

Table 9:

The weight of corroded iron sheet in in the 0.04 M $MgCl_2$ and 0.6 M NaCl solution

System	Ethanol (%)	m_1 (g)	m_2 (g)	m_3 (g)	Average	Error
0.04 M $MgCl_2$	0	8.9399	8.9421	8.9425	8.9415	0.0011
	25	8.9457	8.9483	8.9479	8.9473	0.0007
	50	9.0299	9.0318	9.0318	9.0311	0.0010
	75	9.0848	9.0863	9.0865	9.0858	0.0008
	100	9.1758	9.1777	9.1781	9.1772	0.0011
0.6 M NaCl	0	9.1323	9.1329	9.1324	9.1325	0.0004
	25	9.1087	9.1095	9.1083	9.1088	0.0004
	50	9.0748	9.0758	9.0748	9.0751	0.0004
	75	9.0701	9.0712	9.0703	9.0705	0.0002
	100	8.7606	8.7611	8.7615	8.7610	0.0003

Supplementary Table 9 | The weight of corroded iron sheets, which were semi-immersed in 0.04 M $MgCl_2$ and 0.6 M NaCl solution, respectively.

Table 10:

The corrosion rate of iron sheet in the 0.04 M $MgCl_2$ and 0.6 M NaCl solution

System	Ethanol (%)	m_0 (g)	m_n (g)	corrosion rate ($g.cm^{-2}.h^{-1}$)
0.04 M $MgCl_2$	0	8.3540	8.9415	0.0097
	25	8.3540	8.9473	0.0098
	50	8.3540	9.0311	0.0112
	75	8.3540	9.0858	0.0121
	100	8.3540	9.1772	0.0137
0.6 M NaCl	0	8.3540	9.1325	0.0129
	25	8.3540	9.1088	0.0125
	50	8.3540	9.0751	0.0120
	75	8.3540	9.0705	0.0119
	100	8.3540	8.7610	0.0067

Supplementary Table 10 | The corrosion rate of iron sheets, which were semi-immersed in 0.04 M $MgCl_2$ and 0.6M NaCl solution, respectively.

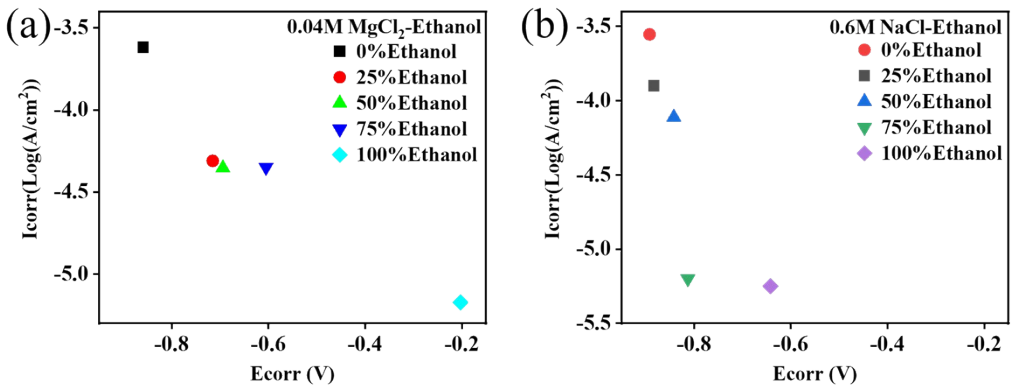

Supplementary Fig. 4 | (a) The Icorr. and Ecorr. of iron in the 0.04M $MgCl_2$ solution, Corresponding respectively to 0, 25, 50, 75 and 100 vol.% ethanol. (b) he Icorr. and Ecorr. iron in the 0.6M NaCl solution, Corresponding respectively to 0, 25, 50, 75 and 100 vol.% ethanol.

Table 11:

The Tafel date of iron in the 0.04 M $MgCl_2$ and 0.6 M NaCl solution

System	Ethanol (%)	Icorr. (A/cm^2)	Ecorr. (V)	AE (%)
0.04M $MgCl_2$	0	-0.859	2.407×10^{-4}	------
	25	-0.715	4.899×10^{-5}	19
	50	-0.694	4.431×10^{-5}	20
	75	-0.605	4.486×10^{-5}	21
	100	-0.203	6.721×10^{-6}	42
0.6 M NaCl	0	-0.883	1.258×10^{-4}	------
	25	-0.892	2.792×10^{-4}	9
	50	-0.842	7.715×10^{-5}	15
	75	-0.813	$6..323\times10^{-6}$	46
	100	-0.642	5.635×10^{-6}	47

Supplementary Table 11 | The Tafel data of iron in the 0.04 M $MgCl_2$ and 0.6 M NaCl solution. The data include corrosion potential (Ecorr.), corrosion current density (Icorr.) and the anticorrosion efficiency (AE%).

Section 5: The SEM-EDS data of oxygen content about corrosion products caused by in 0.04 M $MgCl_2$ solution

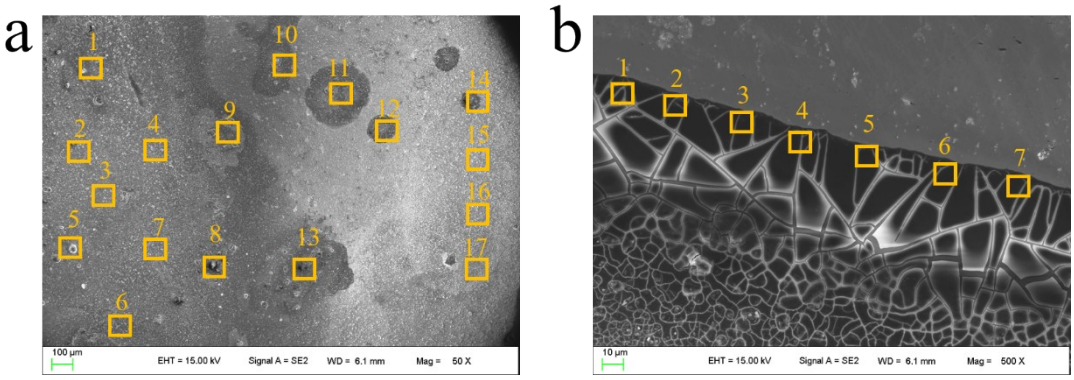

Supplementary Fig. 5 | (a) the SEM image of corrosion product in the liquid phase caused by 0.04 M $MgCl_2$ solution containing ethanol rations from 0 vol.%. (b) the SEM image of corrosion product at the gas-liquid interface caused by 0.04 M $MgCl_2$ solution containing ethanol rations from 0 vol.%.

Table 12:

Count	Oxygen content %
Liquid phase	
1	27.6
2	26.8
3	26.5
4	26.7
5	23.5
6	27.8
7	26.9
8	29.4
9	30.2
10	31.5
11	29.6
12	27.3
13	29.1
14	28.7
15	25.6
16	32.4
17	30.8
Average:	28.2
Errors:	2.20
Interface	
1	10.3
2	11.2
3	10.8
4	8.9

5	8.3
6	9.8
7	8.1
Average:	9.6
Errors:	1.13

Supplementary Table 12 | The percentage of oxygen content about corrosion product caused by 0.04 M $MgCl_2$ solution containing ethanol rations from 0 vol.% in the liquid phase and at the gas-liquid interface.

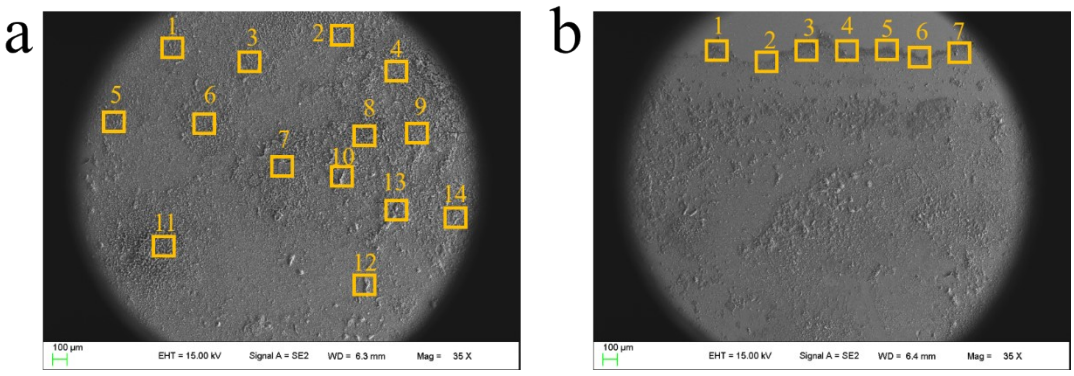

Supplementary Fig. 6 | (a) the SEM image of corrosion product in the liquid phase caused by 0.04 M $MgCl_2$ solution containing ethanol rations from 25 vol.%. (b) the SEM image of corrosion product at the gas-liquid interface caused by 0.04 M $MgCl_2$ solution containing ethanol rations from 25 vol.%.

Table 13:

Count	Oxygen content %
Liquid phase	
1	20.2
2	18.9
3	19.4
4	19.2
5	18.3
6	22.4
7	18.5
8	20.9
9	21.3
10	17.5
11	18.2
12	20.1
13	20.2
14	22.5
Average:	18.3
Errors:	1.38
Interface	
1	18.3
2	22.8
3	21.6

4	21.5
5	22.5
6	20.5
7	20.6
Average:	21.1
Errors:	1.39

Supplementary Table 13 | The percentage of oxygen content about corrosion product caused by 0.04 M $MgCl_2$ solution containing ethanol rations from 25 vol.% in the liquid phase and at the gas-liquid interface.

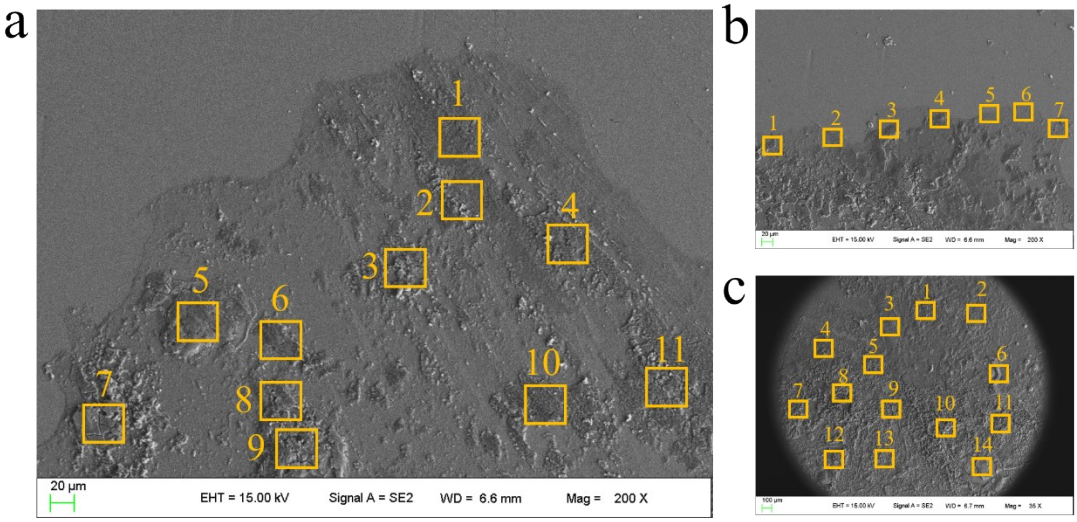

Supplementary Fig. 7 | (a) the SEM image of corrosion product in the gas phase caused by 0.04 M $MgCl_2$ solution containing ethanol rations from 50 vol.%. (b) the SEM image of corrosion product in the liquid phase caused by 0.04 M $MgCl_2$ solution containing ethanol rations from 50 vol.%. (c) the SEM image of corrosion product at the gas phase caused by 0.04 M $MgCl_2$ solution containing ethanol rations from 50 vol.%.

Table 14:

Count	Oxygen content %
Gas phase	
1	29.2
2	28.6
3	32.4
4	33.2
5	30.5
6	29.8
7	31.2
8	32.6
9	29.8
10	30.7
11	27.2
Average:	30.4

Errors:	1.45
Interface	
1	24.5
2	26.3
3	27.1
4	28.2
5	25.3
6	26.4
7	28.7
Average:	26.6
Errors:	1.19
Liquid phase	
1	14.3
2	15.2
3	16.8
4	17.9
5	15.8
6	18.6
7	17.1
8	14.6
9	14.3
10	15.6
11	16.8
12	18.5
13	14.3
14	19.2
Average:	15.3
Errors:	1.66

Supplementary Table 14 | The percentage of oxygen content about corrosion products caused by 0.04 M $MgCl_2$ solution containing ethanol rations from 50 vol.% in the gas phase, liquid phase and at the gas-liquid interface.

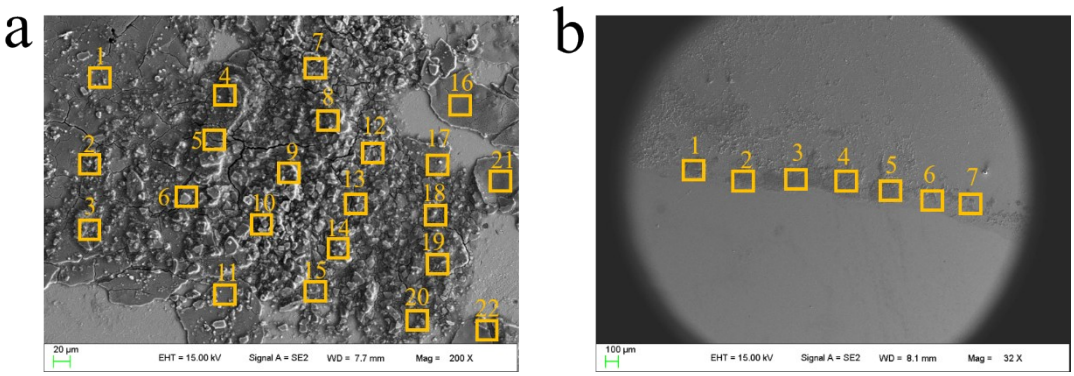

Supplementary Fig. 8 | (a) the SEM image of corrosion product in the liquid phase caused by 0.04 M $MgCl_2$ solution containing ethanol rations from 75 vol.%. (b) the SEM image of corrosion product at the gas-liquid interface caused by 0.04 M $MgCl_2$ solution containing ethanol rations from 75 vol.%.

Table 15:

Count	Oxygen content %
Gas phase	
1	53.3
2	49.5
3	37.6
4	35.4
5	51.6
6	40.3
7	42.3
8	45.3
9	45.8
10	45.5
11	52.8
12	43.4
13	39.8
14	53.8
15	44.9
16	50.8
17	50.3
18	43.2
19	41.6
20	53.3
21	49.5
22	52.6
Average:	41.8
Errors:	5.62
Interface	
1	35.2
2	36.4
3	38.7
4	34.3
5	37.4
6	36.1
7	38.8
Average:	36.7
Errors:	1.57

Supplementary Table 15 | The percentage of oxygen content about corrosion products caused by 0.04 M $MgCl_2$ solution containing ethanol rations from 75 vol.% in the gas phase and at the gas-liquid interface.

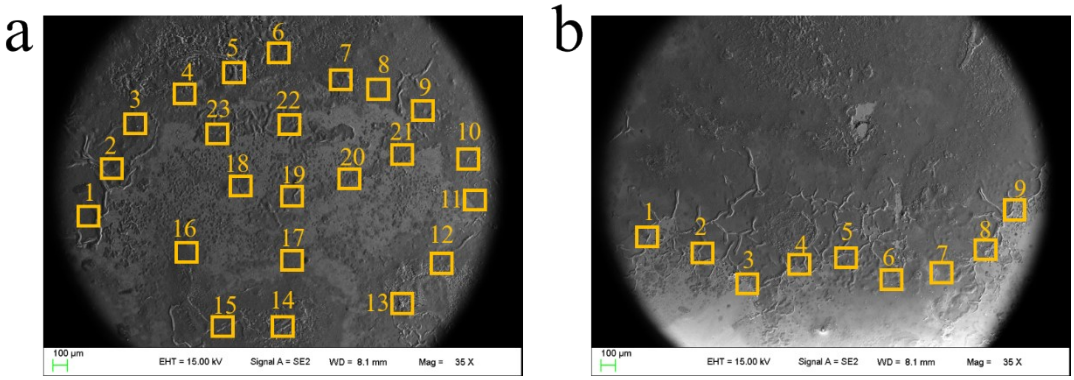

Supplementary Fig. 9 | (a) the SEM image of corrosion product in the liquid phase caused by 0.04 M $MgCl_2$ solution containing ethanol rations from 100 vol.%. (b) the SEM image of corrosion product at the gas-liquid interface caused by 0.04 M $MgCl_2$ solution containing ethanol rations from 100 vol.%.

Table 16:

Count	Oxygen content %
Gas phase	
1	55.4
2	56.8
3	57.2
4	65.6
5	65.3
6	58.8
7	67.4
8	52.8
9	58.7
10	64.9
11	58.5
12	62.6
13	58.3
14	52.4
15	67.6
16	54.9
17	65.2
18	63.1
19	59.4
20	55.4
21	56.8
22	57.2
23	67.2
Average:	52.7
Errors:	4.64
Interface	
1	39.2
2	40.8
3	43.6

4	42.5
5	41.6
6	42.3
7	41.2
8	40.2
9	38.2
Average:	42.7
Errors:	1.59

Supplementary Table 16 | The percentage of oxygen content about corrosion products caused by 0.04 M $MgCl_2$ solution containing ethanol rations from 100 vol.% in the gas phase and at the gas-liquid interface.

Section 6: The SEM-EDS data of oxygen content about corrosion products caused by 0.6 M NaCl solution

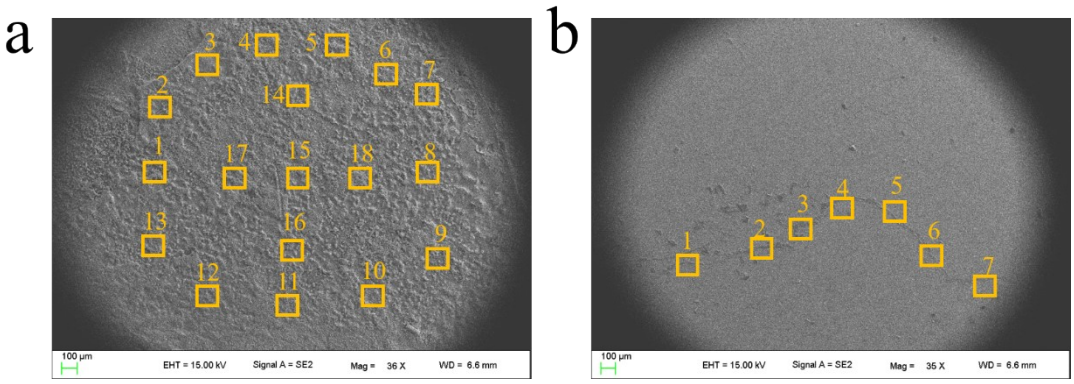

Supplementary Fig. 10 | (a) the SEM image of corrosion product in the liquid phase caused by 0.6 M NaCl solution containing ethanol rations from 0 vol.%. (b) the SEM image of corrosion product at the gas-liquid interface caused by 0.6 M NaCl solution containing ethanol rations from 0 vol.%.

Table 17:

Count	Oxygen content %
Liquid phase	
1	57.4
2	59.6
3	60.3
4	62.1
5	52.4
6	55.3
7	54.6
8	56.7
9	57.2
10	58.9
11	59.1

12	60.3
13	62.4
14	61.4
15	50.3
16	62.4
17	64.3
18	50.3
Average:	58.0
Errors:	3.67
Interface	
1	40.6
2	43.5
3	42.1
4	45.7
5	44.1
6	42.7
Average:	43.1
Errors:	1.59

Supplementary Table 17 | The percentage of oxygen content about corrosion product caused by 0.6 M NaCl solution containing ethanol rations from 0 vol.% in the liquid phase and at the gas-liquid interface.

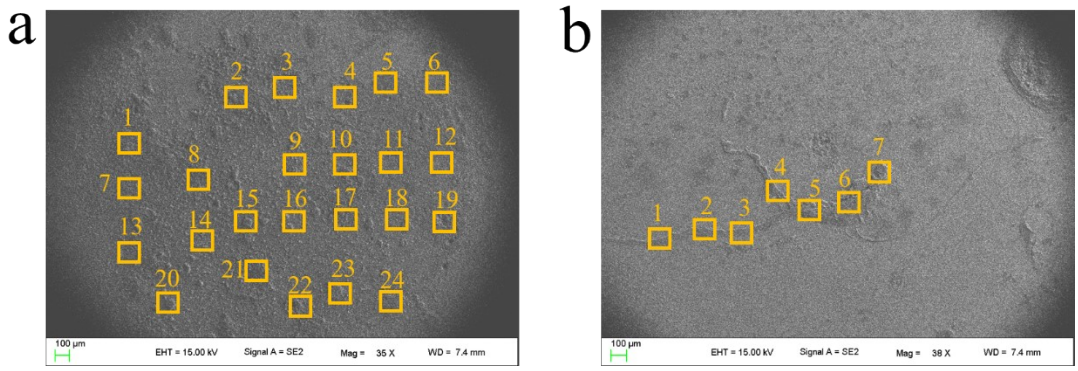

Supplementary Fig. 11 | (a) the SEM image of corrosion product in the liquid phase caused by 0.6 M NaCl solution containing ethanol rations from 25 vol.%. (b) the SEM image of corrosion product at the gas-liquid interface caused by 0.6 M NaCl solution containing ethanol rations from 25 vol.%.

Table 18:

Count	Oxygen content %
Liquid phase	
1	42.5
2	46.3
3	45.1
4	44.6
5	43.2
6	46.3
7	50.1

8	
9	48.9
10	49.2
11	47.3
12	45.2
13	53.1
14	45.2
15	46.3
16	48.9
17	49.6
18	50.9
19	52.6
20	50.4
21	44.3
22	40.1
23	51.8
24	45.6
25	43.6
Average:	47.1
Errors:	3.33
Interface	
1	29.8
2	30.6
3	32.5
4	33.4
5	30.1
6	31.5
7	35.4
Average:	31.9
Errors:	3.33

Supplementary Table 18 | The percentage of oxygen content about corrosion product caused by 0.6 M NaCl solution containing ethanol rations from 25 vol.% in the liquid phase and at the gas-liquid interface.

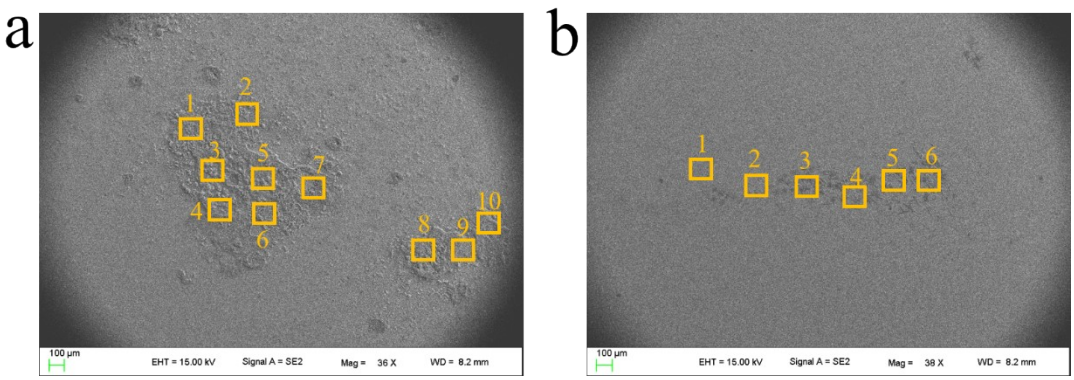

Supplementary Fig. 12 | (a) the SEM image of corrosion product in the liquid phase caused by 0.6 M NaCl solution containing ethanol rations from 50 vol.%. (b) the SEM image of corrosion product at the gas-liquid interface caused by 0.6 M NaCl solution

containing ethanol rations from 50 vol.%.

Table 19:

Count	Oxygen content %
Liquid phase	
1	34.2
2	38.9
3	37.4
4	36.2
5	34.6
6	35.8
7	37.6
8	33.5
9	34.9
10	38.5
Average:	36.1
Errors:	1.77
Interface	
1	20.3
2	21.6
3	23.8
4	24.4
5	25.7
6	20.9
Average:	22.7
Errors:	1.96

Supplementary Table 19 | The percentage of oxygen content about corrosion product caused by 0.6 M NaCl solution containing ethanol rations from 50 vol.% in the liquid phase and at the gas-liquid interface.

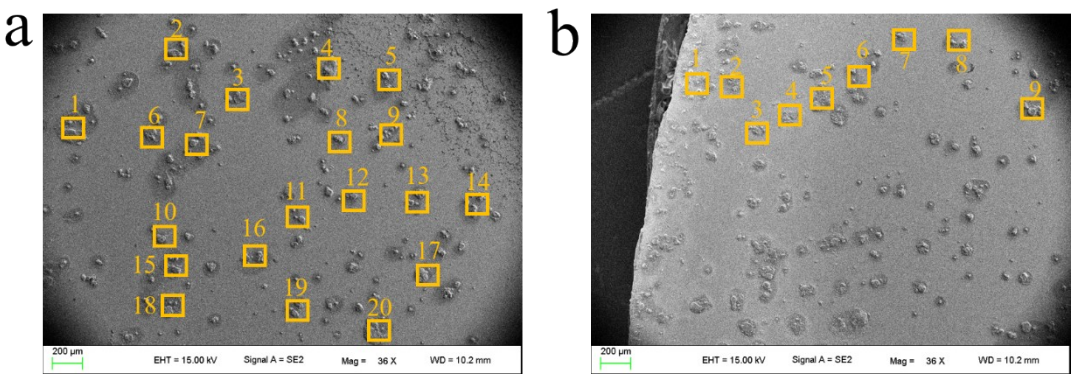

Supplementary Fig. 13 | (a) the SEM image of corrosion product in the liquid phase caused by 0.6 M NaCl solution containing ethanol rations from 75 vol.%. (b) the SEM image of corrosion product at the gas-liquid interface caused by 0.6 M NaCl solution containing ethanol rations from 75 vol.%.

Table 20:

Count	Oxygen content %
Liquid phase	
1	24.5
2	35.6
3	30.2
4	40.5
5	38.5
6	37.4
7	36.3
8	25.4
9	42.1
10	32.4
11	33.6
12	30.6
13	35.6
14	40.9
15	38.4
16	24.5
17	35.6
18	30.2
19	40.5
20	32.6
Average:	27.7
Errors:	5.43
Interface	
1	14.3
2	17.2
3	15.6
4	16.2
5	16.9
6	18.5
7	15.6
8	14.8
9	17.2
Average:	16.2
Errors:	1.24

Supplementary Table 20 | The percentage of oxygen content about corrosion product caused by 0.6 M NaCl solution containing ethanol rations from 75 vol.% in the liquid phase and at the gas-liquid interface.

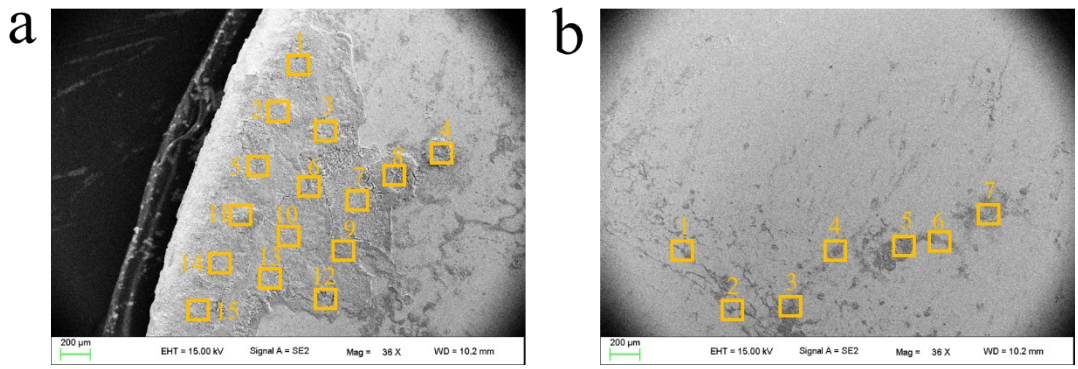

Supplementary Fig. 14 | (a) the SEM image of corrosion product in the gas phase caused by 0.6 M NaCl solution containing ethanol rations from 100 vol.%. (b) the SEM image of corrosion product at the gas-liquid interface caused by 0.6 M NaCl solution containing ethanol rations from 100 vol.%.

Table 21:

Count	Oxygen content %
Gas phase	
1	8.3
2	9.7
3	11.6
4	12.3
5	9.4
6	10.5
7	10.8
8	7.3
9	11.4
10	12.6
11	9.5
12	13.6
13	12.4
14	11.6
15	15.2
Average:	10.3
Errors:	1.63
Interface	
1	22.8
2	23.6
3	25.4
4	26.7
5	27.2
6	25.4
7	23.4
Average:	24.9
Errors:	1.57

Supplementary Table 21 | The percentage of oxygen content about corrosion product caused by 0.6 M NaCl solution containing ethanol rations from 100 vol.% in

the gas phase and at the gas-liquid interface.

Section 7: The SEM and XRD data of corrosion products in the liquid phase and gas phase

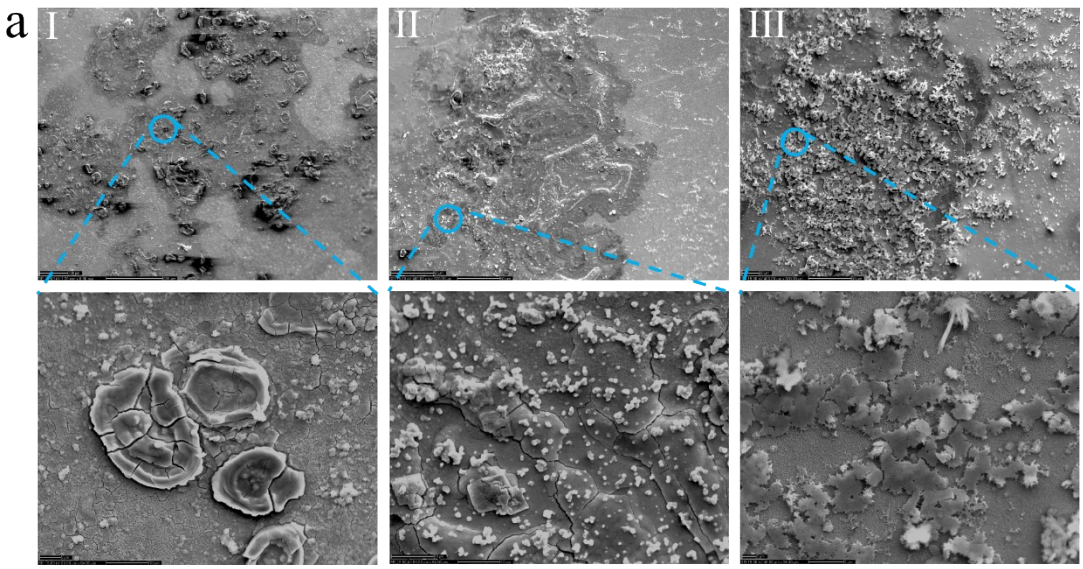

Supplementary Fig. 15 | (a) the SEM image of corrosion products in the liquid phase caused by 0.04 M $MgCl_2$ solution containing ethanol rations from 0 vol.%.

Three representative SEM images are selected from the corrosion products caused by 0.04 mol/L $MgCl_2$ solution contains 0 vol.% ethanol. The blue circle marks the local area of the corroded circular iron sheet, and the corresponding SEM images below the blue dotted line extension is the local enlarged picture of the corroded circular iron sheet.

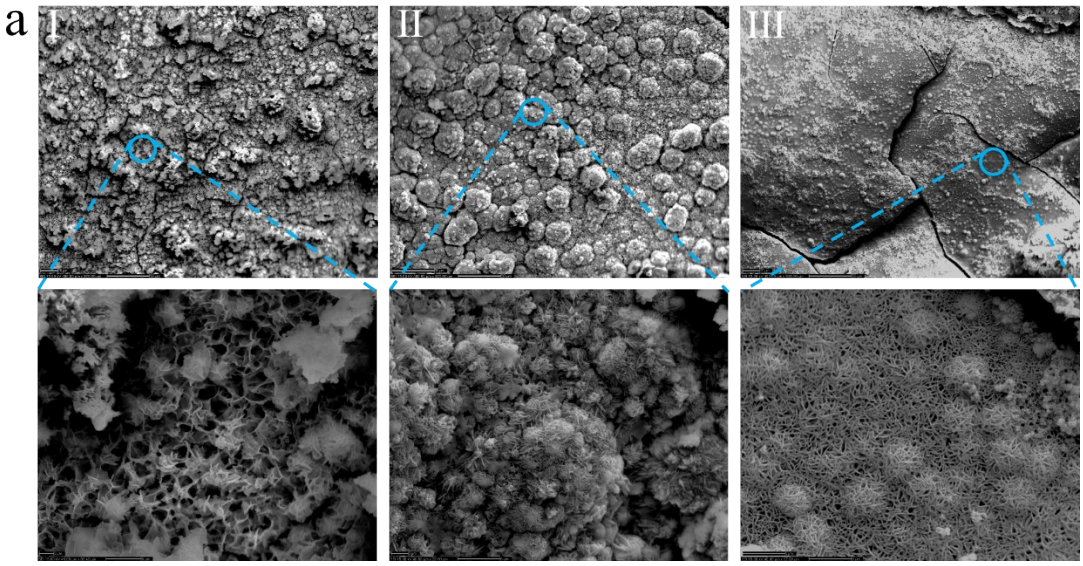

Supplementary Fig. 16 | (a) the SEM image of corrosion products in gas phase caused by 0.04 M $MgCl_2$ solution containing ethanol rations from 75 vol.%.

Three representative SEM images are selected from the corrosion products caused by 0.04 mol/L $MgCl_2$ solution contains 75 vol.% ethanol. The blue circle marks the local area of the corroded circular iron sheet, and the corresponding SEM images below the blue dotted line extension is the local enlarged picture of the corroded circular iron sheet.

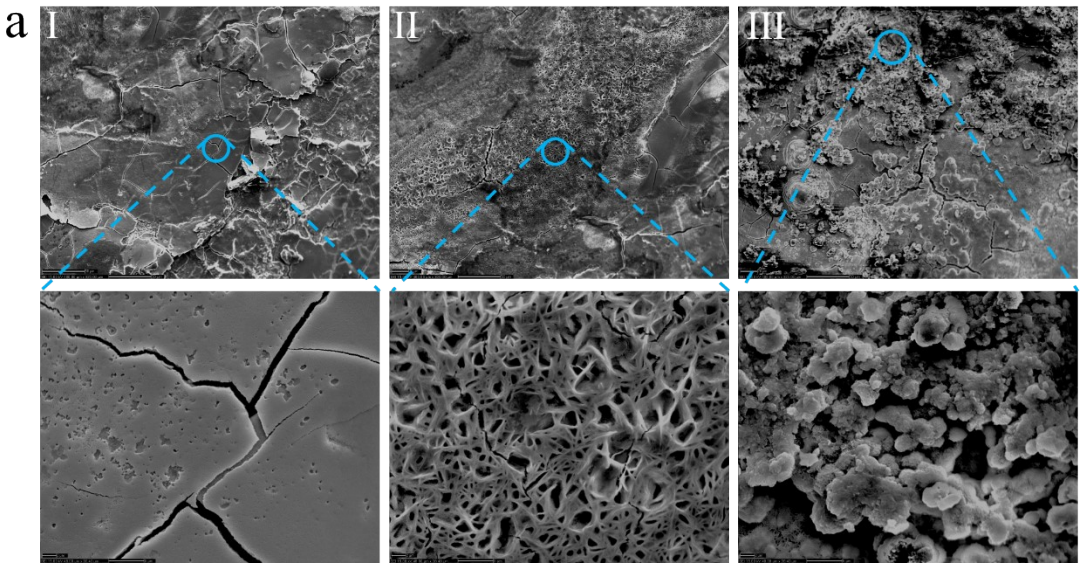

Supplementary Fig. 17 | (a) the SEM image of corrosion products in gas phase caused by 0.04 M $MgCl_2$ solution containing ethanol rations from 100 vol.%.

Three representative SEM images are selected from the corrosion products caused by 0.04 mol/L $MgCl_2$ solution contains 100 vol.% ethanol. The blue circle

marks the local area of the corroded circular iron sheet, and the corresponding SEM images below the blue dotted line extension is the local enlarged picture of the corroded circular iron sheet.

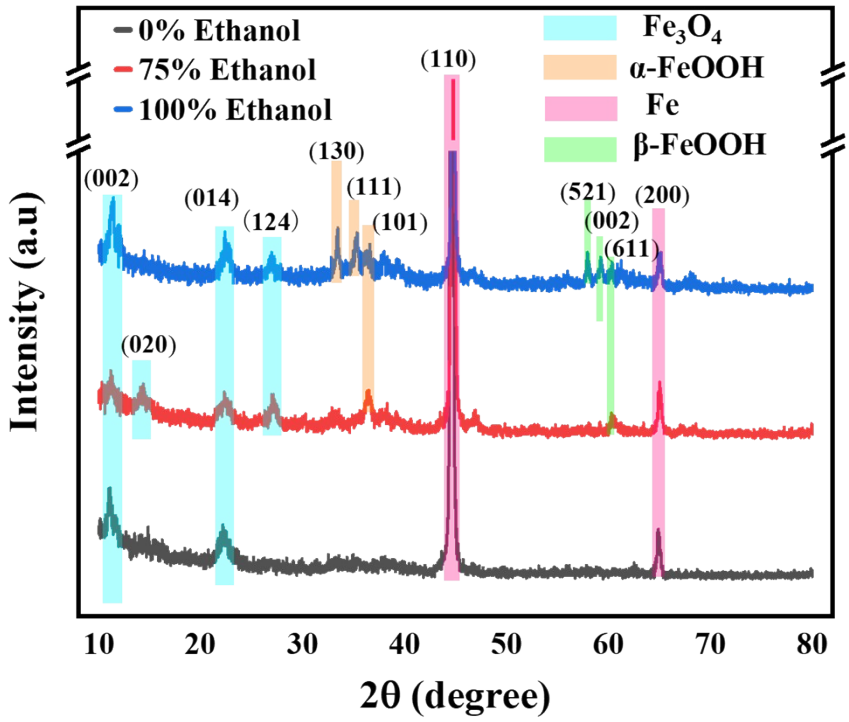

Supplementary Fig. 18 | The XRD image of corrosion products in the liquid phase and gas phase caused by 0.04 M $MgCl_2$ solution containing ethanol rations from 0, 75, and 100 vol.%.

The result of XRD determines Fe_3O_4 in the liquid corrosion products, but with increase of ethanol content, there are more α-FeOOH and β-FeOOH were determined in the gas corrosion products.

In the 0, 75 and 100 vol.% ethanol, the Bragg peaks indices belonging to Fe_3O_4 corresponding to (002), (020), (014) and (124), respectively. In the 75 and 100 vol.% ethanol, the Bragg peaks indices belonging to α-FeOOH corresponding to (130), (111) and (101), respectively. The Bragg peaks indices belonging to β-FeOOH corresponding to (521), (002) and (611), respectively.

Section 8: The XPS and SEM-EDS data of corrosion products in the gas phase

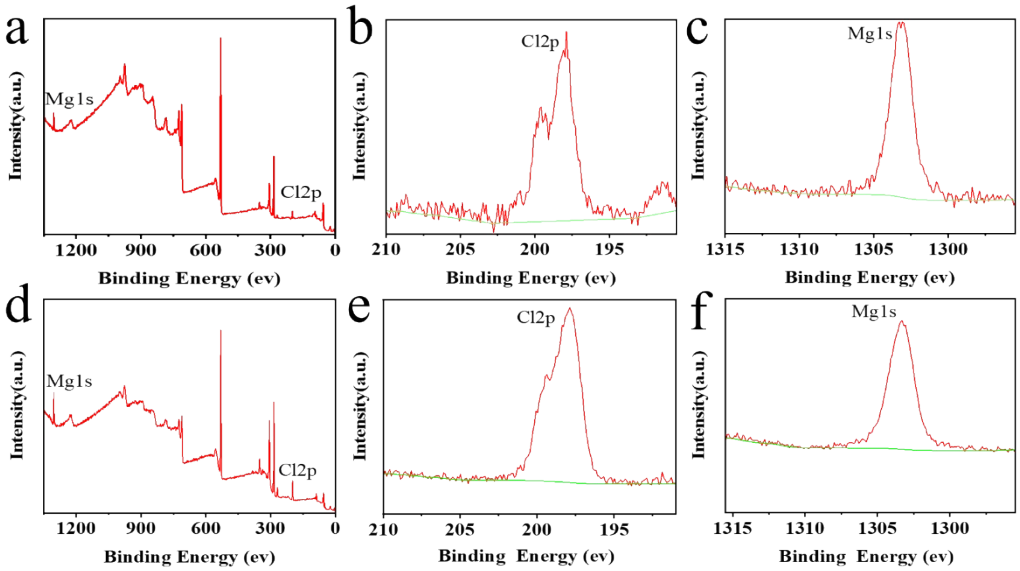

Supplementary Fig. 19 | The XPS image of corrosion products in the gas phase caused by 0.04 M $MgCl_2$ solution containing ethanol rations from 75 and 100 vol.%, receptively. (**a**)-(**c**): corrosion products caused by 0.04 M $MgCl_2$ solution containing ethanol rations from 75 vol.%. (**a**) XPS for all elements. **(b)** XPS for Cl2p part. (**c**) XPS for Mg1s part. (**d**)-(**f**): corrosion products caused by 0.04 M $MgCl_2$ solution containing ethanol rations from 100 vol.%. (**d**) XPS for all elements. **(e)** XPS for Cl2p part. (**f**) XPS for Mg1s part.

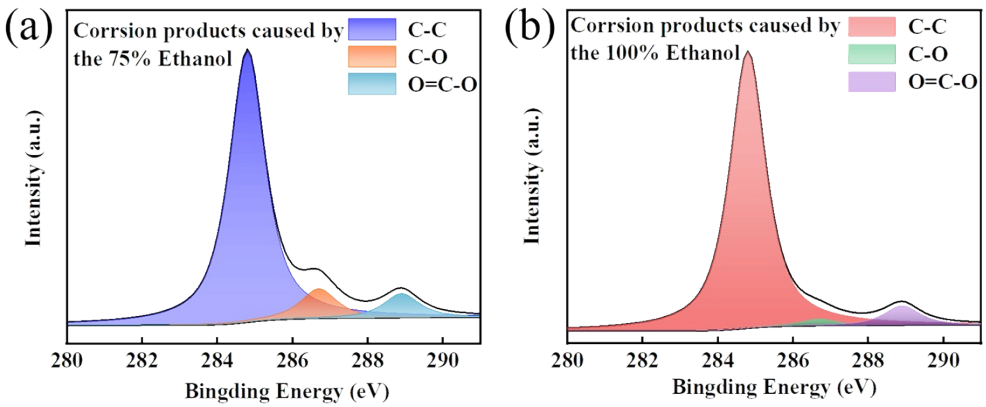

Supplementary Fig. 20 |The X-ray photoelectron spectrometer spectra of C1s. **(a)** Corrosion products caused by 75 vol.% ethanol of $MgCl_2$ solution. **(b)** Corrosion products caused by 100 vol.% ethanol of $MgCl_2$ solution.

As shown in the Figure 20(a-b), the deconvoluted C1s spectra were divided into three peaks at binding energies of 284.8, 286.7, 288.9 eV, which corresponding with C-C, C-O and O=C-O,[7, 8] respectively. In the corrosion products caused by the 75 and 100 vol.% ethanol, we all found the chemical bonds of C-O. The chemical bond of C-O was contributed to the ethanol. In the $MgCl_2$ solution, excluding the presence of the known peaks of carbon contamination, we still find proof of the presence of ethanol. By processing the XPS spectra of C1s, this identified ethanol as the trigger for corrosion products in the gas phase.

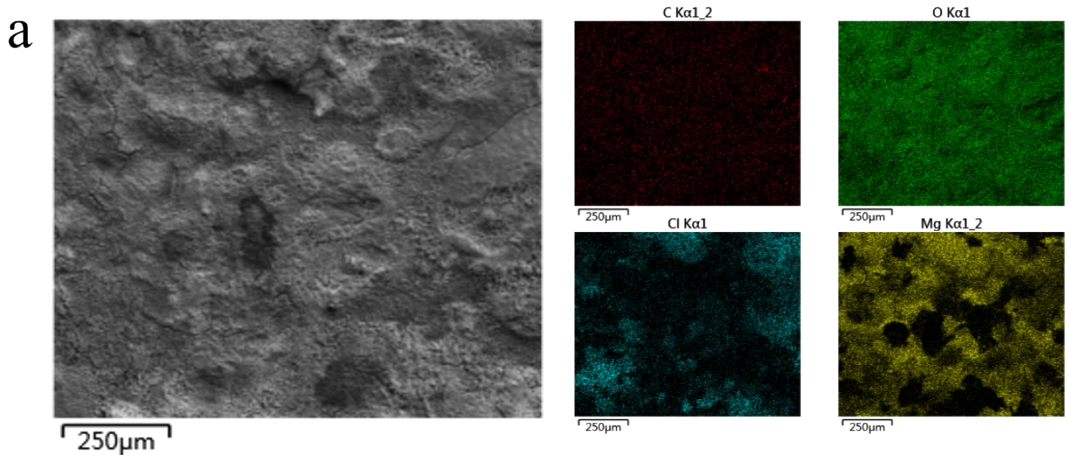

Supplementary Fig. 21 | (a) The SEM-EDS image of corrosion products in the gas phase caused by 0.04 M $MgCl_2$ solution containing ethanol rations from 75 vol.%.

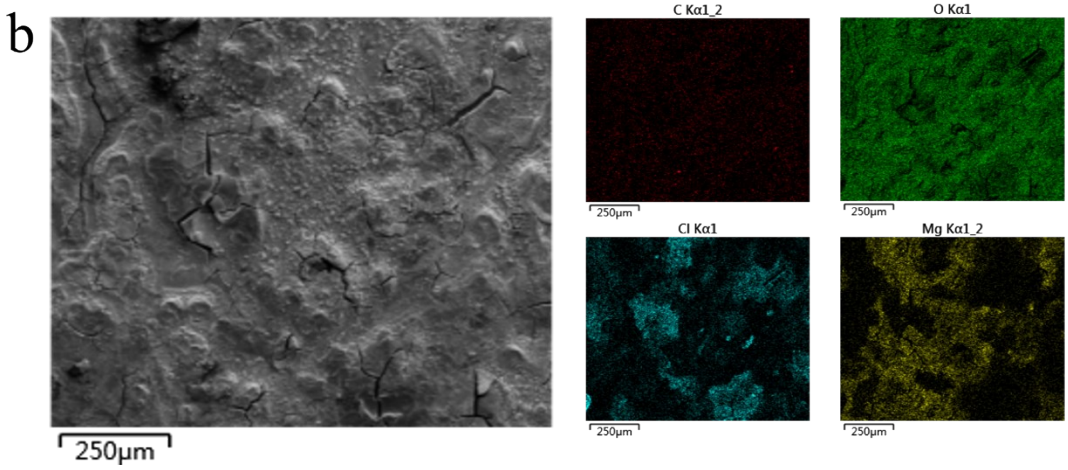

Supplementary Fig. 22 | (b) The EDS image of corrosion products in the gas phase caused by 0.04 M $MgCl_2$ solution containing ethanol rations from 100 vol.%.

Reference

S1. P. Han, C. Chen, H. Yu, Y. Xu and Y. Zheng, *Corros. Sci.*, 2016, **112**, 128-137.

S2. A. D. K. I. Weeraratne, C. C. Hewa-Rahinduwage, L. Luo and C. N. Verani, *Langmuir*, 2020, **36**, 14173-14180.

S3. W. Li, Y. Jiang, D. Liu, J. Zhu, Y. Xie and L. Liu, *Coatings*, 2021, **11**.

S4. Y. Qiu, X. Tu, X. Lu and J. Yang, *Corros. Sci.*, 2022, **199**.

S5. M. Finsgar, *Corros. Sci.*, 2020, **169**.

S6. X. Q. Cheng, Z. Jin, M. Liu and X. G. Li, *Corros. Sci.*, 2017, **115**, 135-142.

S7. M. Cui, S. Ren, H. Zhao, Q. Xue and L. Wang, *Chem. Eng. J.*, 2018, **335**, 255-266.

S8. R. Yi, R. Yang, R. Yu, J. Lan, J. Chen, Z. Wang, L. Chen and M. Wu, *Rsc Advances*, 2019, **9**, 40397-40403.